

A neutron star with a carbon atmosphere in the Cassiopeia A supernova remnant

Wynn C. G. Ho ^{*} & Craig O. Heinke [†]

^{*} School of Mathematics, University of Southampton, Southampton, SO17 1BJ, United Kingdom.

[†] Department of Physics, University of Alberta, Room 238 CEB, 11322-89 Avenue, Edmonton, AB, T6G 2G7, Canada.

The surface of hot neutron stars is covered by a thin atmosphere. If there is accretion after neutron star formation, the atmosphere could be composed of light elements (H or He); if no accretion takes place or if thermonuclear reactions occur after accretion, heavy elements (for example, Fe) are expected. Despite detailed searches, observations have been unable to confirm the atmospheric composition of isolated neutron stars.¹ Here we report an analysis of archival observations of the compact X-ray source in the centre of the Cassiopeia A supernova remnant. We show that a carbon atmosphere neutron star (with low magnetic field) produces a good fit to the spectrum. Our emission model, in contrast with others,^{2–4} implies an emission size consistent with theoretical predictions for the radius of neutron stars. This result suggests that there is nuclear burning in the surface layers^{5,6} and also identifies the compact source as a very young (≈ 330 -year-old) neutron star.

Cassiopeia A is one of the youngest-known supernova remnants in the Milky Way and is at a distance of $d = 3.4_{-0.1}^{+0.3}$ kiloparsecs (kpc) from the Earth.⁷ The supernova that gave rise to the remnant may have been observed by John Flamsteed in 1680 (ref. 8); the implied age coincides with estimates made by studying the expansion of the remnant.⁹ Although the supernova remnant is extremely well-studied, the central compact source was only identified in first-light Chandra X-ray observations.¹⁰ (We shall refer to the compact source as Cas A.)

We considered archival Chandra X-ray Observatory data from two studies of Cas A, both using the ACIS-S charge-coupled device which provides spatial and spectral information.¹¹ A series of Chandra observations, totalling 1 megasecond, was performed in 2004 to study the supernova remnant¹²; these are referred to here as the Hwang data. A shorter (70 kiloseconds) observation in 2006 was designed to study the compact source, here referred to as the Pavlov data.⁴ Figure 1 shows the Cas A spectra, as well as our carbon model fit.

We fitted the Hwang and Pavlov data simultaneously with several models: a blackbody, a H atmosphere,¹³ and atmospheres composed of pure He, C, N, or O; these are illustrated in Fig. 2. To identify promising models, the mass and radius of the atmosphere models were fixed to the canonical neutron star values of $M_{\text{NS}} = 1.4M_{\text{Sun}}$ and $R_{\text{NS}} = 10$ km, where M_{Sun} is the solar mass. The normalization factor, which can be interpreted as the fraction of the surface that is emitting X-ray radiation, was left free. The results are given in Table 1.

The H, He, and C atmospheres provided good fits to the data (somewhat better than the blackbody). However, the derived sizes of the emission region R for H and He

(4 km and 5 km, respectively) are much smaller than the theoretical size of a neutron star R_{NS} (~ 10 km; ref. 14). This would suggest the emission region is a hot spot on the neutron star surface, which would probably result in X-ray pulsations as the hot spot rotated with the star. However, these pulsations have not been detected.^{4,15} Fits to the data were performed using an additional (temperature) component, for example, a second blackbody or atmosphere spectrum, which produced inferred R^∞ of ≈ 0.2 and 2 km for blackbody fits or 0.4 and 11 km for H atmosphere fits.⁴ The high-temperature component has been interpreted as being due to a small hot polar cap, while the low-temperature component is due to emission from the remaining cooler neutron star surface. However, it is difficult to generate, through anisotropic heat conduction, such small regions of high-temperature contrast on the neutron star surface.¹⁶ Also, the two temperature regions would again probably produce (undetected) X-ray pulsations. On the other hand, by considering a C atmosphere, we derived an emission size $R \approx 12 - 15$ km that closely matches the theoretical prediction for the radius of a neutron star $R_{\text{NS}} \sim 10 - 14$ km.¹⁴ In this case, the X-ray observations are detecting emission from the entire stellar surface, and therefore the emission would not necessarily vary as the star rotates (although local temperature differences could cause small brightness fluctuations on top of the bright background). Thus we conclude that Cas A is consistent with a low-magnetic field carbon atmosphere neutron star of mass $1.4M_{\text{Sun}}$, radius 12–15 km, and surface temperature $T = 1.8 \times 10^6$ K.

Interpreting the size of the emission region to be the true neutron star radius ($R = R_{\text{NS}}$), we can constrain the neutron star mass M_{NS} and radius R_{NS} by using a range

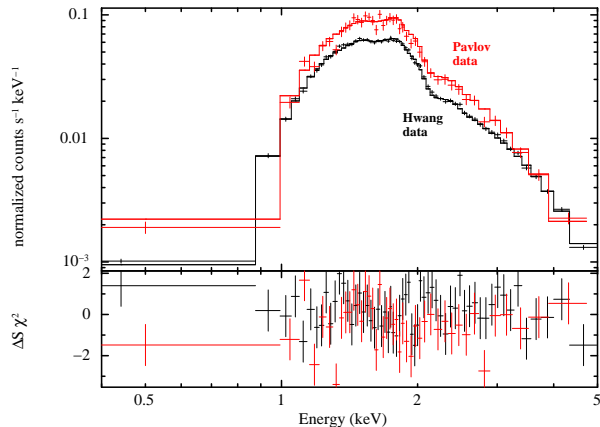


Figure 1. Chandra X-ray spectra of Cas A. Spectra from the Hwang (black) and Pavlov (red) observations and fits with our C spectral model. Error bars are 1 s.d. The lower panel shows the fit residuals $\Delta S\chi^2$ in units of s.d. The Hwang observations place Cas A off-axis (blurring Chandra’s point-spread function), and the high count-rate of Cas A distorts the spectrum through detection of multiple photons during one 3.04-s frame-time (known as pile-up²⁴). The Pavlov observation is performed in a special instrument configuration to reduce the frametime to 0.34 s (thus reducing pile-up) and places Cas A at the position of best focus.⁴ We used the level 2 event files provided by the Chandra Data Archive and performed data reduction and analysis with CIAO 4.1 and XSPEC 12.4.0. Owing to the slightly distorted shape of the Cas A point-spread function in the Hwang data, we extracted the source spectra using an elliptical region of dimensions 1.23 by 1.72 arcsec, rotated to match the position angle of the point-spread function ellipticity, and the background from a surrounding annulus of 2.19 to 4.37 arcsec. Alternative extraction methods produce similar results. We combine the spectra and responses to make a single, deep spectrum of Cas A. For the Pavlov data, we extract the Cas A spectrum and the nearby background following the procedure of ref. 4. The spectra are binned to achieve at least 1,000 counts per bin for the Hwang data and 140 counts per bin for the Pavlov data. X-ray and bolometric luminosities are $L_X(0.5\text{-}10\text{ keV}) = 4.3 \times 10^{33}$ ergs s⁻¹ and $L_{\text{bol}} = 7.0 \times 10^{33}$ ergs s⁻¹, respectively.

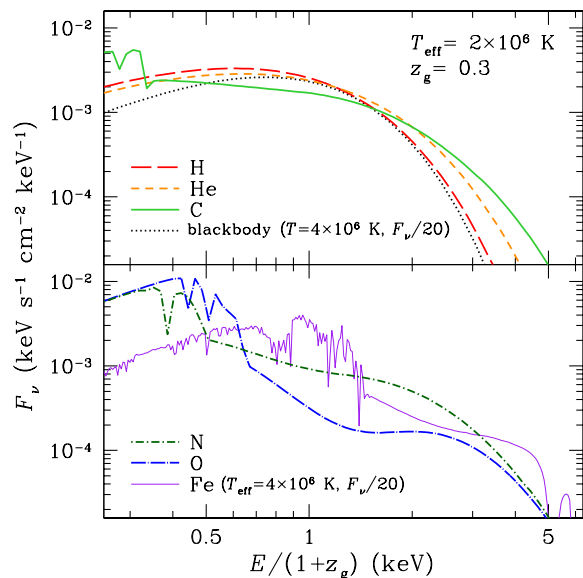


Figure 2. Model atmosphere spectra. Energy flux F_ν for atmospheres with H, He, C, N, O, and Fe and a blackbody. The energy has been redshifted by $1 + z_g = (1 - 2GM_{\text{NS}}/c^2 R_{\text{NS}})^{-1/2} = 1.3$, where z_g is the gravitational redshift, and the flux has been scaled by $(10\text{ km}/3.4\text{ kpc})^2$. Our models are constructed assuming a plane-parallel atmosphere (because the atmosphere thickness of $\sim 1\text{ cm}$ is much smaller than the stellar size) that is in hydrostatic and radiative equilibrium with constant gravitational acceleration $g = (1 + z_g) GM_{\text{NS}}/R_{\text{NS}}^2$. The efficient separation of light and heavy elements results in atmospheres composed of a single element.²⁵ The opacities are obtained from tables computed by the Opacity Project.²⁶ (The energy range of the tables covers $E/kT \sim 0.07 - 20$. When opacities are required beyond this range, we use the E^{-3} -dependence of free-free and bound-free absorption; this approximation has a minor effect, except for the Fe model, which is shown for illustrative purposes.) Light-element atmospheres generate spectra that are harder than blackbodies (at the same temperature) because of the energy-dependence of the opacity,^{27,28} so atmospheric spectral fits result in temperatures that are lower and sizes that are larger compared to those obtained using blackbody spectra. Further details of the atmosphere model construction are given in ref. 29. When $B \ll 2.35 \times 10^9 Z^2\text{ G}$ ($\sim 8 \times 10^{10}\text{ G}$ for carbon), magnetic-field effects on the radiation transport and atoms in the atmospheric plasma are negligible.^{27,28} Previous works found poor fits to the data using magnetic ($B \geq 10^{12}\text{ G}$) H atmosphere spectra,^{2,4} while magnetic mid- Z element spectra are similar to low-magnetic field Fe spectra in that they are blackbody-like in shape and contain many lines.³⁰

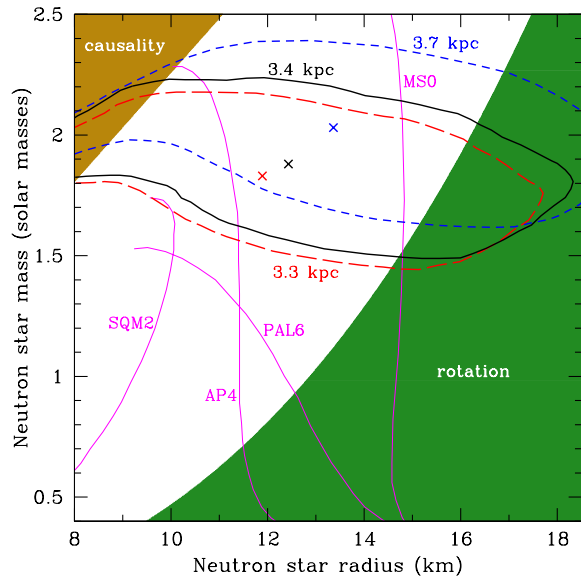


Figure 3. Neutron star mass and radius. 90% confidence contours of χ^2 around the best-fitting Cas A mass and radius (crosses) for distances of 3.3 kpc (red long-dashed line), 3.4 kpc (thick black solid line), and 3.7 kpc (blue short-dashed line). The upper-left and lower-right regions are excluded by constraints from the requirement of causality and from the fastest-rotating neutron star known.¹⁴ The thin magenta solid lines represent predictions for the masses and radii of neutron stars using different theoretical models (labelled SQM2, AP4, PAL6, and MS0) of the neutron star interior.¹⁴

of surface gravity models. If we fix $M_{\text{NS}} = 1.4M_{\text{Sun}}$ and the distance to Cas A as $d = 3.4$ kpc (ref. 7), then we find a surface effective temperature $T_{\text{eff}} = 1.61^{+0.14}_{-0.05} \times 10^6$ K and emission size $R = 15.6^{+1.3}_{-2.7}$ km. Figure 3 shows 90% confidence contours in mass and radius when both are allowed to vary. The contours for distances between 3.3 and 3.7 kpc constrain $M_{\text{NS}} \approx 1.5 - 2.4M_{\text{Sun}}$ and $R_{\text{NS}} \approx 8 - 17$ km. The mass constraint, significantly above the canonical $1.4M_{\text{Sun}}$, suggests a moderately stiff nuclear equation of state.¹⁴

The emission of neutrinos determines the thermal evolution of a neutron star at ages $\lesssim 10^5$ y. The particle reactions that contribute to this emission are determined by the state of the matter, which is strongly dependent on the total mass of the star.^{17,18} Owing to the small uncertainties in the temperature and age of Cas A, as well as our measured mass, Cas A can be used to constrain matter properties in the stellar interior. More importantly, because the next youngest neutron stars for which surface thermal emission has been measured have ages exceeding a few thousand years, Cas A (with an age of only about 330 years) serves as a valuable window into the early life of a passively-cooling neutron star. Previously, the utility of Cas A in studying the thermal evolution was hindered

by the fact that the measured temperature (taken to be from a local hot spot because $R \ll R_{\text{NS}}$) could only be used to set an upper limit on the average surface temperature.² However, with our T_{eff} and L_{bol} (which are surface averages given that $R = R_{\text{NS}}$), detailed comparisons with theoretical models^{17–19} can now be made.

The presence of a carbon atmosphere on the surface is probably a consequence of the youth of Cas A. The surface of newly-formed neutron stars is uncertain; it is thought to be composed of an element between O and Fe, depending on which layers of the pre-supernova star fall back onto the proto-neutron star²⁰; this fallback material could also form light elements through spallation.⁶ Over time, the surface accumulates an overlying layer of light elements by accretion from the circumstellar medium (although this can be countered by pulsar-wind excavation⁶). Fits to the thermal radiation from older neutron stars do indeed suggest H or He atmospheres at $10^4 - 10^5$ years and heavy-element (blackbody-like) atmospheres at $\gtrsim 10^5$ years.¹ However, the picture is incomplete for young neutron stars ($t \lesssim 10^4$ y). At a depth just below the surface, the temperature (and density) is conducive to nuclear burning ($T \gtrsim 10^8$ K). Accreted material diffuses to this layer and is rapidly consumed, with depletion of H in $\lesssim 1$ y and He in $\lesssim 100$ y.^{5,6} This process of diffusive nuclear burning is very temperature-sensitive; as the neutron star cools, the temperature drops below the threshold needed for the material to be burned, and a light-element atmosphere can begin to build up after $10^4 - 10^6$ y (ref. 6).

Cas A is the youngest of a class of neutron stars that are located near the centre of supernova remnants, possess steady long-term fluxes and soft thermal spectra, and have no detectable pulsar wind nebulae or radio pulsations.¹ X-ray pulsations have been detected in three members of this class, with periods of tenths of seconds. Timing measurements suggest that they have (dipolar) magnetic fields $B \ll 10^{12}$ G (ref. 21). If the field of Cas A is $\sim (1 - 5) \times 10^{11}$ G, then a spectral feature due to the electron cyclotron resonance may appear in the Chandra energy range, but this has yet to be detected. The lack of a visible pulsar wind nebula and no indication of magnetospheric activity (such as radio or gamma-ray emission or a high-energy hard power-law component), like those seen in classical pulsars (with $B \gtrsim 10^{12}$ G), also suggest the magnetic field is low. The weak surface magnetic field inferred for this class would have important implications for the neutron star population. These objects could be representative of the early life of neutron stars before becoming classical pulsars. In this case, either neutron star magnetic fields develop by a dynamo mechanism, or else a strong field (produced during the collapse of the progenitor star) is buried and has not yet emerged.²² These objects could also form a distinct group of low magnetic field neutron stars, which never manifest pulsar-like behaviour; this would suggest a large population of old, cool, unobserved sources. Finally, we note that the detection of the

hydrogen-like C edge at about 0.45 keV (unredshifted), in similar sources with less intervening gas and dust than Cas A has, would not only provide further evidence for carbon atmospheres but also give a measurement of the gravitational redshift.

Received 21 July; accepted 15 September 2009.

1. Pavlov, G. G., Zavlin, V. E., & Sanwal, D. in Proc. Vol. 270 WE-Heraeus Seminar: Neutron Stars, Pulsars and Supernova Remnants (eds Becker, W., Lesch, H., & Trümper, J.) 273–286 (MPE Rep. 278, MPI, Garching, 2002).
2. Pavlov, G. G., Zavlin, V. E., Aschenbach, B., Trümper, J., & Sanwal, D. The compact central object in Cassiopeia A: a neutron star with hot polar caps or a black hole?. *Astrophys. J.* **531**, L53–L56 (2000).
3. Chakrabarty, D., Pivovarov, M. J., Hernquist, L. E., Heyl, J. S., & Narayan, R. The central X-ray point source in Cassiopeia A. *Astrophys. J.* **548**, 800–810 (2001).
4. Pavlov, G. G. & Luna, G. J. M. A dedicated Chandra ACIS observation of the central compact object in the Cassiopeia A supernova remnant. *Astrophys. J.* **703**, 910–921 (2009).
5. Rosen, L. C. Hydrogen and helium abundances in neutron-star atmospheres, *Astrophys. & Sp. Sci.* **1**, 372–387 (1968).
6. Chang, P., & Bildsten, L. Evolution of young neutron star envelopes. *Astrophys. J.* **605**, 830–839 (2004).
7. Reed, J. E., Hester, J. J., Fabian, A. C., & Winkler, P. F. The three-dimensional structure of the Cassiopeia A supernova remnant. I. The spherical shell. *Astrophys. J.* **440**, 706–721 (1995).
8. Ashworth, W. B. A probable Flamsteed observation of the Cassiopeia A supernova. *J. Hist. Astron.* **11**, 1–9 (1980).
9. Fesen, R. A., et al. The expansion asymmetry and age of the Cassiopeia A supernova remnant. *Astrophys. J.* **645**, 283–292 (2006).
10. Tananbaum, H. Cassiopeia A. *IAU Circ. No.* 7246 (1999).
11. Garmire, G. P., Bautz, M. W., Ford, P. G., Nousek, J. A., & Ricker, G. R. Advanced CCD imaging spectrometer (ACIS) instrument on the Chandra X-ray Observatory. *Proc. SPIE* **4851**, 28–44 (2003).
12. Hwang, U., et al. A million second Chandra view of Cassiopeia A. *Astrophys. J.* **615**, L117–L120 (2004).
13. Heinke, C. O., Rybicki, G. B., Narayan, R., & Grindlay, J. E. A hydrogen atmosphere spectral model applied to the neutron star X7 in the globular cluster 47 Tucanae. *Astrophys. J.* **644**, 1090–1103 (2006).
14. Lattimer, J. M. & Prakash, M. Neutron star observations: prognosis for equation of state constraints. *Phys. Rep.* **442**, 109–165 (2007).
15. Murray, S. S., Ransom, S. M., Juda, M., Hwang, U., & Holt, S. S. Is the compact source at the center of Cassiopeia A pulsed?. *Astrophys. J.* **566**, 1039–1044 (2002).
16. Greenstein, G. & Hartke, G. J. Pulselike character of blackbody radiation from neutron stars. *Astrophys. J.* **271**, 283–293 (1983).
17. Yakovlev, D. G. & Pethick, C. J. Neutron star cooling. *Annu. Rev. Astron. Astrophys.* **42**, 169–210 (2004).
18. Page, D., Geppert, U., & Weber, F. The cooling of compact stars. *Nucl. Phys. A* **777**, 497–530 (2006).
19. Tsuruta, S., et al. Thermal evolution of hyperon-mixed neutron stars. *Astrophys. J.* **691**, 621–632 (2009).
20. Woosley, S. E., Heger, A., & Weaver, T. A. The evolution and explosion of massive stars. *Rev. Mod. Phys.* **74**, 1015–1071 (2002).
21. Gotthelf, E. V. & Halpern, J. P. Discovery of a 112 ms X-ray pulsar in Puppis A: Further evidence of neutron stars weakly magnetized at birth. *Astrophys. J.* **695**, L35–L39 (2009).
22. Muslimov, A. & Page, D. Delayed switch-on of pulsars. *Astrophys. J.* **440**, L77–L80 (1995).
23. Predehl, P., Costantini, E., Hasinger, G., & Tanaka, Y. XMM-Newton observation of the galactic centre - evidence against the X-ray reflection nebulae model?. *Astronomische Nachrichten* **324**, 73–76 (2003).
24. Davis, J. E. Event pileup in charge-coupled devices. *Astrophys. J.* **562**, 575–582 (2001).
25. Alcock, C. & Illarionov, A. Surface chemistry of stars I. Diffusion of heavy ions in white dwarf envelopes. *Astrophys. J.* **235**, 534–540 (1980).
26. The Opacity Project Team, “The Opacity Project”, <http://cdsweb.u-strasbg.fr/topbase/op.html> (2009).
27. Rajagopal, M. & Romani, R. W. Model atmospheres for low-field neutron stars. *Astrophys. J.* **461**, 327–333 (1996).
28. Zavlin, V. E., Pavlov, G. G., & Shibano, Yu. A. Model neutron star atmospheres with low magnetic fields. *Astron. Astrophys.* **315**, 141–152 (1996).
29. Ho, W. C. G. & Lai, D. Atmospheres and spectra of strongly magnetized neutron stars. *Mon. Not. R. Astron. Soc.* **327**, 1081–1096 (2001).
30. Mori, K. & Ho, W. C. G. Modelling mid-Z element atmospheres for strongly magnetized neutron stars. *Mon. Not. R. Astron. Soc.* **377**, 905–919 (2007).

Acknowledgements. W.C.G.H. thanks N. Badnell, P. Chang, and D. Lai for discussions. W.C.G.H. appreciates the use of the computer facilities at the Kavli Institute for Particle Astrophysics and Cosmology. W.C.G.H. acknowledges support from the Science and Technology Facilities Council (STFC) in the United Kingdom. C.O.H. acknowledges support from the Natural Sciences and Engineering Research Council (NSERC) of Canada.

Author Contributions W.C.G.H. calculated the new models and wrote the manuscript. C.O.H. reduced the data, fitted the models to the data, and contributed to the manuscript.

Author Information Reprints and permissions information is available at www.nature.com/reprints. The authors declare no competing financial interests. Correspondence and requests for materials should be addressed to W.C.G.H. (wynnho@slac.stanford.edu) or C.O.H. (cheinke@phys.ualberta.ca).

Atmosphere model	N_{H} (10^{22} cm^{-2})	kT (eV)	Normalization	$\chi^2/\text{d.o.f.}$	Null hypothesis probability (%)
Hydrogen	$1.65^{+0.04}_{-0.05}$	241^{+7}_{-6}	$0.18^{+0.03}_{-0.03}$	106.3/99	29
Helium	$1.62^{+0.04}_{-0.05}$	228^{+9}_{-8}	$0.22^{+0.05}_{-0.04}$	112.4/99	17
Carbon	$1.73^{+0.05}_{-0.04}$	155^{+7}_{-6}	$1.84^{+0.56}_{-0.42}$	105.3/99	31
Nitrogen	1.37	172	1.18	388/99	0
Oxygen	1.03	234	0.20	2439/99	0
Blackbody model	$1.46^{+0.04}_{-0.04}$	$kT^{\infty} = 387^{+7}_{-6} \text{ eV}$	$R^{\infty} = 1.0^{+0.1}_{-0.1} \text{ km}$	134.2/98	11

Table 1. X-ray spectral fitting of Cas A. Joint fit results to the Hwang and Pavlov data with neutron star atmosphere and blackbody models that are modified by photoelectric absorption N_{H} (using the Tübingen-Boulder absorption routine TBABS with wilms model abundances in the X-ray spectral fitting package XSPEC; see <http://heasarc.gsfc.nasa.gov/docs/xanadu/xspec/index.html>), dust scattering,²³ and corrections for pile-up²⁴ (the grade migration parameter of the pile-up algorithm is allowed to float freely and is 0.36 for the best-fit C model). Chandra data with such high statistics reveals systematic uncertainties in the Chandra calibration,¹³ so we added a systematic uncertainty of 3% in quadrature. All parameter errors are given at 90% confidence. Errors are not reported when the reduced $\chi^2 > 2$. The normalization refers to the fraction of the neutron star surface emitting radiation (for a 10 km stellar radius and 3.4 kpc distance). The null hypothesis probability is the probability that one realization of the model fit to the data would have a reduced χ^2 greater than that obtained; less than 5% indicates a poor fit. $T^{\infty} = T/(1 + z_{\text{g}})$ and $R^{\infty} = R(1 + z_{\text{g}})$ are the temperature and radius measured by an observer at infinity, and d.o.f. is the number of degrees of freedom.